Tiered Digital Twin-Assisted Cooperative Multiple Targets Tracking

Zhou, Longyu; Leng, Supeng; Wang, Qing; Ming, Yujun; Liu, Qiang

DOI
10.1109/TWC.2023.3311035

Publication date
2023

Document Version
Final published version

Published in
IEEE Transactions on Wireless Communications

Tiered Digital Twin-Assisted Cooperative Multiple Targets Tracking

Longyu Zhou, *Student Member, IEEE*, Supeng Leng, *Member, IEEE*, Qing Wang, *Senior Member, IEEE*, Yujun Ming, and Qiang Liu, *Member, IEEE*

***Abstract*— The development of the intelligent Internet of Things has facilitated the adoption of high-efficiency Multiple Targets Tracking (MTT) in many civil security applications. However, existing MTT technologies cannot offer full capability in accurate and real-time MTT for civil security. Many attractive applications in the next-generation wireless network, like Unmanned Aerial Vehicle (UAV) swarm, are envisioned to be exploited for enhanced MTT with the advantage of flexibility. Nonetheless, highly dynamic moving targets impose some new challenges. UAVs cannot always perform expected cooperative tracking in conventional architectures as well. To address these problems, we design a tiered Digital Twin-assisted tracking framework in this paper, which leverages multi-grained imitation for real-time and accurate MTT. We imitate a coarse-grained MTT to ensure a high successful tracking ratio. We then design a fine-grained imitation with a reaction-diffusion mechanism to explore the feasible cooperators based on trajectory prediction. Hardware-in-the-loop simulations demonstrate that our tiered framework can reduce 66.7% of the system latency overhead compared to the conventional DDPG benchmark while improving the successful tracking ratio by 30.6%.**

***Index Terms*— Tiered imitation, digital twin, UAV swarm, target tracking.**

I. Introduction

With the rapid development of the intelligent Internet of Things (IoT), Unmanned Aerial Vehicles (UAVs) have gradually become one of the particular applications in the next-generation wireless networks. The main driving forces behind this are low manufacturing costs, versatility, and high flexibility. The advantages of UAV lie in the possibility of addressing the increasing requirements of civil and commercial applications such as disaster rescue, equipment inspection, and precision agriculture [1], [2]. With the aid of Artificial Intelligence (AI), UAV swarm-empowered Multiple Targets Tracking (UAV-MTT) applications have elicited a growth in cooperatively tracking diverse mobile targets in many complicated scenarios, including space exploration and regional security [3]. For instance, a UAV swarm can cooperate to detect mobile targets to ensure the safety of security systems in complex surveillance environments. The relevant information is collected and transmitted to a remote center for target detection and trajectory estimation. The estimation results can guide UAVs to track those mobile targets.

However, a UAV-MTT system lacks tracking efficiency with the terminal-cloud structure due to remote physical distance between the end devices and the servers in the cloud [4]. In the context of time-critical MTT, the terminal-cloud architecture cannot meet the real-time tracking requirement. Furthermore, the out-of-date tracking decisions might cause UAVs to associate with improper targets, degrading the system's efficiency. It can lead to unpredictable physical collisions among UAVs with overlapped tracking paths. On the other side, many high-speed moving targets with time-varying trajectories can easily elude UAV observations to cause a low successful tracking ratio. Thus, it is essential to propose a real-time cooperative UAV-MTT solution for harsh MTT environments.

The long transmission latency can be reduced using the terminal-edge architecture [5]. Nevertheless, the latency of tracking decisions on edge servers may be unacceptable due to their limited computing capability. As one of the critical enablers for 6G networks, AI technology can digest a large amount of data [6]. AI-based schemes can assist UAVs in learning and acquiring tracking experiences as a data training tool for cooperative tracking. Unfortunately, policy-based or value-based learning approaches for optimal tracking decisions usually lead to a considerable system convergence latency because of the frequent iterations [4]. It cannot effectively cope with the previously mentioned challenge of high mobility.

As one of the emerging technologies, Digital Twin (DT) can accurately estimate the MTT environments based on the data interaction mapping a physical element to a virtual entity. The virtual entity can be operated by digital twin models based on the data from the physical environments. It can implement high-efficiency target analysis and tracking diagnosis. However, it is time-consuming to imitate the entire MTT process with abundant targets sensed by the UAVs. The

Manuscript received 27 September 2022; revised 2 March 2023, 30 May 2023, and 31 July 2023; accepted 29 August 2023. Date of publication 8 September 2023; date of current version 11 April 2024. This work was supported in part by the National Natural Science Foundation of China under Grant 62171104. The associate editor coordinating the review of this article and approving it for publication was H. Chen. *(Corresponding author: Supeng Leng.)*

Longyu Zhou, Supeng Leng, and Yujun Ming are with the School of Information and Communication Engineering, University of Electronic Science and Technology of China (UESTC), Chengdu 611731, China, and also with the Shenzhen Institute for Advanced Study, UESTC, Shenzhen 518000, China (e-mail: zhoulyfuture@outlook.com; spleng@uestc.edu.cn; mingyujun112@gmail.com).

Qing Wang is with the Computer Science Department, Delft University of Technology, 2628 XE Delft, The Netherlands (e-mail: qing.wang@tudelft.nl).

Qiang Liu is with the Yangtze Delta Region Institute (Quzhou), University of Electronic Science and Technology of China, Quzhou, Zhejiang 324000, China (e-mail: liuqiang@uestc.edu.cn).

Color versions of one or more figures in this article are available at https://doi.org/10.1109/TWC.2023.3311035.

Digital Object Identifier 10.1109/TWC.2023.3311035

quantity of MTT imitation iterations is dramatically increased with the number of targets. It may also result in resource misallocation to imitate different speeds of the targets. It indicates a need to develop a tiered DT-assisted tracking framework with terminal-edge-cloud cooperation for the high-efficiency MTT systems.

In this paper, we design a tiered DT-assisted tracking framework through the cooperation of the terminals, edge, and cloud. It can also operate smoothly without the cloud. The framework enables to perform a high-efficiency MTT with joint coarse- and fine-grained imitations. The coarse-grained imitation provides suitable associations among UAVs and targets for accurate MTT. Moreover, group leaders are dynamically selected to perform fine-grained imitation for real-time MTT. The main contributions are summarized below.

- We propose a tiered DT-assisted tracking framework to perform accurate and real-time MTT. Unlike traditional terminal-edge-cloud architectures with centralized management, the tiered DT framework is the first exploration of the multi-grained cooperative MTT system. Explicitly, the cloud server with a coarse-grained DT imitation can dynamically assign target observation and tracking missions to different UAV groups during the tracking process. Moreover, these group leaders provide a real-time tracking performance based on a fine-grained DT imitation. In addition, our framework can still smoothly operate the MTT system in a distributed cooperative manner when the cloud server is unavailable.
- To conduct an effective coarse-grained imitation, we design a flexible inter-group cooperative MTT system that can work well either with or without the support of a cloud server. In the case of an available cloud server, the server adaptively divides the UAV swarm into multiple groups and make optimal tracking associations among targets and groups for accurate MTT. When the cloud server is absent, the UAV swarm can autonomously implement the coarse-grained imitation and dynamically form a suitable number of groups to associate time-varying targets based on their attributes. Moreover, in both cases, UAV groups can wait to cooperatively track high-mobility targets by elastically adjusting observation ranges. The inter-group cooperative tracking can significantly improve the successful tracking ratio.
- To track mobile targets in real-time, the fine-grained DT-based imitation operated by group leaders provides a lightweight imitation service according to the target information. Specifically, group leaders can guide proper UAV members to track low-speed moving targets cooperatively. It can eliminate significant communication overheads by controlling the number of involved neighbors. In addition, group leaders can imitate UAVs to implement directional information diffusion according to target attributes so that remote cooperators can be invited to track high-speed moving targets based on trajectory prediction sequentially. The flexible fine-grained imitation with intra-group cooperation can reduce tracking latency and enhance the successful tracking ratio.

The rest is organized as follows. The background and related work are given in Section II. Section III gives the system model. The objectives are in Section IV. The tracking algorithm is presented in Section V. Section VI provides the evaluation results. Finally, Section VII concludes this paper.

II. Background and Related Work

A. Background

We first present some background information about UAV-MTT and DT.

1) UAV-MTT: In a UAV-MTT system, multiple UAVs take off for security inspection. UAVs can flexibly fly over a detection area to sense suspicious targets [7]. Fig. 1 shows the flow diagram of a typical UAV-MTT system. Explicitly, UAVs can fly to patrol based on given instructions (*UAV inspection*). The onboard sensors sense multiple moving targets (*target sensing*). The cloud server processes the sensed information (*information collection*). The trajectories are predicted when target behaviors are suspicious (*trajectory prediction)*. The cloud server distributes tracking decisions (*tracking scheduling*). The *advantage* of the UAV-MTT system is that a single UAV can sense multiple targets simultaneously with flexible mobility. Meantime, the natural superiority leads to the *disadvantage* of physical collisions during the tracking process.

2) Digital Twin: A typical digital twin architecture involves three main components [8]: *physical entity, virtual entity, and connected interface*. The physical entity can acquire environmental information, MTT information, and historical tracking experience. The data are fed into the virtual entity based on the connected interface to imitate the real MTT scenario. It can assist the MTT system in avoiding potential incorrect tracking decisions.

B. Related Work

In recent years, many works have focused on UAV swarm-enabled MTT with particular merits such as flexibility and miniaturization. Based on the steps shown in Fig. 1, we present and summarize the state-of-the-art studies in this subsection.

1) UAV Inspection and Target Sensing: UAVs are acquired to cover and sense the maximal detection area with dynamic flight paths for accurate sensing. The authors in [9] constructed a multi-UAV path planning model to implement the target sense. The results demonstrate that the algorithm improved the search efficiency. To remove the restriction of offline area coverage, the authors in [10] used an information theory method to ensure global sensing with desired headings. These studies are effective with the assumption of collision avoidance.

2) Data Collection and Trajectory Prediction: To collect large volumes of target information, the authors in [11] proposed a novel framework that enables UAVs to acquire sensory data. The NP-hard problem can be solved using a heuristic algorithm. With the approximate information, the authors in [12] studied UAV swarm-based antenna arrays using beam-forming technology to exploit the position errors on the Angle-of-Arrival (AoA) estimation. The authors in [13] proposed a rendezvous algorithm which was an opportunistic yet disciplined data delivery scheme. It can improve trajectory prediction accuracy while the latency overhead may be unacceptable.

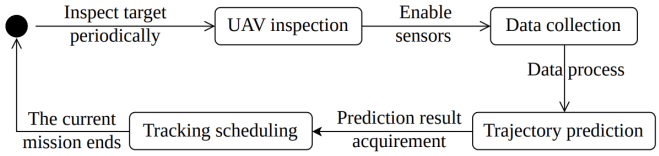

Fig. 1. General procedure of an Unmanned Aerial Vehicle-based Multiple Targets Tracking (UAV-MTT) system.

3) Tracking Scheduling: To improve the tracking performance, the authors in [14] proposed a fuzzy logic and flocking control approach to provide sensor nodes trajectory formation for target tracking. Considering the tracking in an underwater scenario, the authors in [15] proposed a novel cooperative tracking scheme to track underwater moving targets autonomously. However, the researches mainly focus on the target features while ignoring the cooperation among UAVs.

The UAV-MTT above works mainly focus on effective tracking under the assumption of flexible cooperation capability among UAVs. Nonetheless, many UAVs may associate the same target with significantly low tracking performance in the practical MTT scenario. The ineffective UAV allocation makes the low response latency challenging for tracking many targets in complicated environments. A tiered cooperative tracking pattern may be feasible to ensure a high successful tracking ratio in real-time tracking.

III. System Model

This section presents the proposed tiered DT-assisted framework for cooperative tracking.

We take a security and protection application as a typical instance, as illustrated in Fig. 2 with K mobile targets such as unlicensed drones. To avoid the risk, a cloud server in a data center guides M UAVs to monitor and track the K mobile targets. The set of UAV swarm is defined as $\mathcal{M} = \{1, 2, \cdots, M\}$ and the mobile targets are denoted as $\mathcal{K} = \{1, 2, \cdots, K\}$. With the advantage of a macro-view of the cloud, we exploit the cloud to perform a coarse-grained imitation that can decompose the UAV swarm into multiple groups to associate dynamic targets. It can also dynamically allocate UAVs to associate mobile targets in real-time cooperatively. To ensure an accurate MTT, each UAV group conducted by an elected leader can implement a fine-grained imitation based on the velocities and postures of the targets. On the other hand, when the cloud is unreachable, the UAV swarm can implement the coarse-grained imitation using our proposed distributed swarm decomposition algorithm. The main notations are listed in Table I.

In the tiered framework, the coarse-grained imitation is implemented with information of the group leaders and data of the sensed targets. Fine-grained imitation is enabled with the target information from onboard sensors. We describe our framework in three parts: 1) Information collection and transmission. 2) Data processing and trajectory prediction. 3) Tracking imitation.

A. Information Collection and Transmission

To ensure real-time information collection, we provide a cooperative data collection and exchange method inspired by [16]. It can allow UAVs to utilize their sensing resources for acquiring heterogeneous *target information*, including the number of targets, their postures, sizes, and velocities for smooth MTT implementation. The method also integrates computing and communication resources of UAVs to improve communication quality based on power control and channel gains. Besides, UAVs can use the method to select feasible neighbors for large-sized information exchanges among UAVs. On the other hand, neighboring UAVs can send lightweight feedback data after the information-exchanging operation, which can use to estimate and optimize the information exchange performance. We denote the successful sensing probability $P_{i,k}$ of UAV i sensing target k with q: sensors [17]:

$$P_{i,k}(d_{i,k}|q) = 1 - (1 - e^{-bd_{i,k}})^q \geq P_{\min}, \tag{1}$$

where b is used to estimate the sensing quality that is usually set as 1.1; $d_{i,k}$ is the physical distance between UAV i and target k; $P_{\min}$ is the minimal acceptable successful sensing probability. It can collect complete data with effective sensing performance for an accurate tracking imitation. The longest physical sensing distance $d_{i,k,\max}$ is derived as

$$d_{i,k,\max} = \frac{-\ln\left(1 - \sqrt[q]{1 - P_{\min}}\right)}{b}. \tag{2}$$

UAVs can adjust their geographic positions to maintain physical distances less than the $d_{i,k,\max}$ with targets for effective data collection. UWB and ultrasonic sensors collect information on the environment and targets. We know that different types of sensors have different information collection rates. The sensing latency is represented as $t^s_{i,k} = \max_w \frac{q^w_{i,k}}{\lambda_w}$, where λ_w is the sensing rate of sensor w; $q^w_{i,k}$ is the acquired data (bytes) from sensor w for target k. The DT model can conduct UAVs to transmit sensed information based on WiFi-6 protocol with up-to-date beamforming technology. The transmission latency is formulated as $t^c_i = \frac{\sum_{w=1}^{W} q^w_{i,k}}{r_i}$. The transmission rate $r_{i,j}$ is given by [18]

$$r_{i,j} = B(A)\log_2\left(1 + \frac{a_i^{f_i} P_{\text{total}} G_{\text{ma}}(c_i)\hat{e} d_{i,j}^{-\alpha}}{\hat{T} + \bar{T} + a_i^{f_i}\sigma^2}\right), \tag{3}$$

where A is the number of antennas; $B(A)$ is the channel bandwidth; P_{total} is the total transmission power of antennas; $\hat{T} = \sum_{l_j \in \hat{\Omega}_j} G_{\text{ma}}(c_j)L(l_j)e_j$ is the interference received from UAV i with beams pointing towards the UAV j; $L(l_j)$ is captured channel gain function with the spatial distribution density l_j of UAV j; $\bar{T} = \sum_{c_j \in \bar{\Omega}_j} G_{s_j}(c_j)L(l_j)g_j$ is the

TABLE I
List of Used Main Notations in This Work

Notation	Description
$\mathcal{M}$	Set of UAVs
$\mathcal{K}$	Set of mobile targets
$P_{i,k}$	Successful sensing probability of UAV i sensing target k
$r_{i,j}$	Transmission ratio from UAV i to j
h_i	Feature information of UAV i
$d^P_{\max}$	The maximal acceptable prediction error for mobile targets
$E_{\max}$	The maximal energy budget for UAVs
$d_{i,j}$	Physical distance between UAV i and j
$\jmath$	Successful tracking ratio

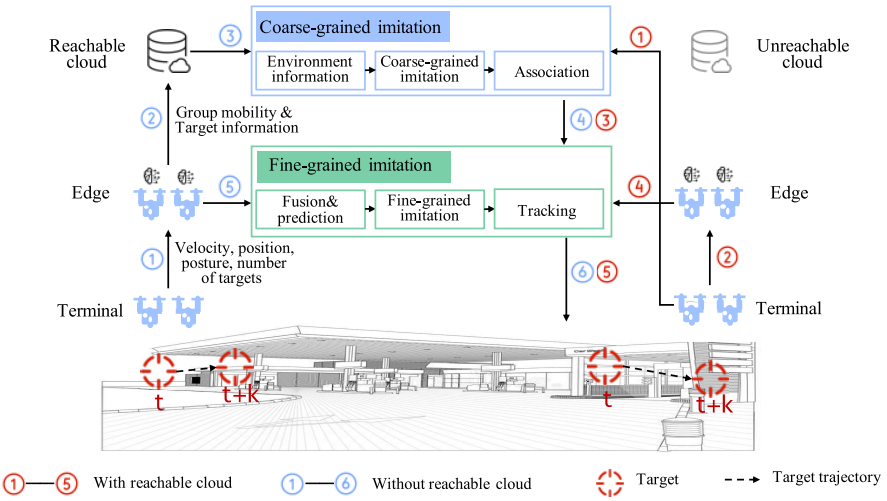

Fig. 2. Illustration of the proposed tiered DT-assisted tracking framework.

interference with beams pointing away from the UAV j; G_{ma} denotes the gains of the main lobe, and $G_{s_j}(c_j)$ denotes the side lobe with the spatial distribution density c_j of UAV j, respectively. G_{ma} is assumed to be non-decreasing while G_{s_j} are non-increasing [19]; $\hat{\Omega}_j$ and $\bar{\Omega}_j$ are sets of interfering UAV j in the sight of the main lobe and side lobe, respectively. $\hat{e}$, e_j, and g_j are random variables capturing the small-scale fading of the link $a_i^{f_i}$, interfering links with beams pointing towards the UAV j, and away from the UAV j, respectively; $d_{i,j} = \sqrt{(x_i - x_j)^2 + (y_i - y_j)^2 + (z_i - z_j)^2}$ is the physical distance between the two UAVs; $a_i^{f_i} \in \{0, 1\}$ is the assigned channel index with spectrum f_i; $\sigma \sim N(0, \delta)$ is the zero mean Gaussian random variables with a standard deviation of δ. In this case, UAVs can adjust beams of A antennas using the WiFi-6 protocol to improve the transmission rate for information exchange in the complicated tracking environment. The high-efficiency transmission ensures a real-time imitation.

The cloud or UAV group leaders can process the heterogeneous data to decompose the UAV swarm into multiple groups for optimal associations among UAVs and targets based on the target information. Furthermore, group leaders can transmit self-position information in real-time to the cloud for coarse-grained tracking imitation in a centralized cooperation mode. Inversely, group leaders can exchange self-position information in a distributed cooperation mode.

B. Data Processing and Trajectory Prediction

The heterogeneous data is processed and integrated as attribute information of UAVs for the decomposition operation. At each time slot t, UAV topology is abstracted to a graph $G(V, E)$, where V is the set of UAVs; E is the set of edges connecting two UAVs; $E_{i,j} = 0$ if the physical distance of UAV i and j is longer than the practical communication range; $E_{i,j} = 1$, otherwise. The target information is embedded into V based on graph learning theory. The feature h_i of UAV i with target information is represented as $h_i = \{a_{i,t}, v_{i,t}, p_{i,t}, d_{i,k}, a_{k,t}, a_{k,t+1}, v_{k,t}, p_{k,t}\}$, where $a_{i,t}$, $v_{i,t}$ and $p_{i,t}$ are the spatial position, moving velocity and posture of UAV i, respectively; $d_{i,k}$ is the physical distance between UAV i and target k; $a_{k,t}$, $v_{k,t}$, and $p_{k,t}$ are the spatial position, moving velocity and posture of the target k, respectively; $a_{k,t+1}$ denotes the position of the target k at time slot $t + 1$. The feature of corresponding edge $h_{i,j}$ is represented as $h_{i,j} = \{d_{i,j}, I_{i,j}\}$, where $I_{i,j}$ is an indicator that $I_{i,j} = 1$ when target k are simultaneously sensed by UAV i and j, $I_{i,j} = 0$, otherwise.

Based on the acquired information, we propose a graph learning-based swarm decomposition algorithm to associate diverse targets in Section V. However, it cannot effectively predict the trajectories of the targets. We invoke the Unscented Filter algorithm to estimate targets' movements. Instead of frequent information collection, the prediction mechanism can significantly ensure real-time imitation in the MTT system (will be detailed in Section IV). However, the UAV topology is dynamic so that UAVs associate with a different number of neighbors, which does not meet the translation invariance [20]. We leverage the graph learning algorithm to implement the coarse-grained tracking imitation.

C. Tracking Imitation

The group leaders can imitate to implement sequential tracking for high-mobility targets. When the targets escape from the current area, the coarse-grained DT can select feasible UAVs to implement re-decomposition for the sequential target tracking (details are in Section V-A). UAVs collect the sensing data frequently using sensors for fine-grained imitation which causes high communication overhead. We design a reaction-diffusion method in the fine-grained imitation only with target information. UAVs can independently imitate to explore the optimal tracking associations based on information exchange with one-hop neighbors. The imitation time is also reduced to output the MTT results in real time (details are in Section V-B).

IV. Problem Formulation

Based on the proposed framework, this section formulates an MTT optimization model. The model targets optimizing the low-latency and accurate MTT under the constraints of power, energy consumption, and sensing performance.

A. Analysis of Latency and Trajectory Prediction

Based on (3), we formulate the latency constraint of target sensing and information exchange:

$$\sum_{k=1}^{K} t_{i,k}^{s} + t_i^{c} \le t_{i,\max}, \tag{4}$$

where $t_{i,\max}$ is the maximal acceptable sensing and communication latency. The constraint guarantees UAVs to perform real-time target sensing and low-latency information exchange for accurate MTT imitation in the virtual world and cooperative tracking in the physical world. The motion of target k is defined as $x_k(t+1) = f_k(t, x_k(t), v(t))$ with a motion estimation model $z_k(t) = h_k(t, x(t), w(t))$, where $x_k(t)$ is the position coordinate of the target k; $v(t)$ and $w(t)$ are zero mean noises that obey the Gaussian distribution, respectively; $f_k(t, x_k(t), v(t))$ is a state transform vector. The state estimation vector and covariance matrix are denoted as $\hat{x}_k(t)|_{x_k(t)}$ and $P_k(t)$. The sampling is given by

$$x_k^{(i+n)}(t)|_{x_k(t)} = \hat{x_k}(t)|_{x_k(t)} - \sqrt{(n+\kappa)P_k(t)}_i \omega^{(i+n)}, \tag{5}$$

where κ is the scaling factor; $\omega^{(i+n)}$ is the weight of the $(i+n)^{\text{th}}$ sampling point; P_k, a symmetric matrix, is a covariance matrix that denotes the posterior estimation of the state vector [21]. $\sqrt{(n+\kappa)P_k(t)}_i$ is either the ith column or the ith row of $(n+\kappa)P_k(t)$: it is the ith row of $(n+\kappa)P_k(t)$ if $\sqrt{(n+\kappa)P_k(t)}_i = A^T A$; and it is the ith column of $(n+\kappa)P_k(t)$ if $\sqrt{(n+\kappa)P_k(t)}_i = AA^T$.

The prediction results are represented as $\hat{x}(t+1|t) = \sum_{i=0}^{2n} \omega^{(i)} \hat{x}^{(i)}(t+1|t)$. Then, the state prediction covariance is updated as $P(t+1|t) = \sum_{i=0}^{2n} \omega^{(i)} [\hat{x}(t+1|t) - \hat{x}^{(i)}(t+1|t)][\hat{x}(t+1|t) - \hat{x}^{(i)}(t+1|t)]^T$. The weighted average value is inferred as $\hat{z}(t+1|t) = \sum_{i=0}^{2n} \omega^{(i)} \hat{z}^{(i)}(t+1|t)$, where $\hat{z}^{(i)}(t+1|t) = h(t+1, \hat{x}^{(i)}(t+1|t))$; $h(\cdot)$ is the nonlinear observation vector. The measurement covariance is $S(t+1) = \sum_{i=0}^{2n} \omega^{(i)} [\hat{z}(t+1|t) - \hat{z}^{(i)}(t+1|t)][\hat{z}(t+1|t) - \hat{z}^{(i)}(t+1|t)]^T$. The system gain is deduced as $W(t+1) = \{\sum_{i=0}^{2n} \omega^{(i)} [\hat{x}(t+1|t) - \hat{x}^{(i)}(t+1|t)][\hat{z}(t+1|t) - \hat{z}^{(i)}(t+1|t)]\} S(k+1)^{-1}$. The trajectory prediction is then represented as $x_i^p = \hat{x}(t+1|t) + W(t+1)[z(t+1) - \hat{z}(t+1|t)]$. The prediction constraint is

$$\|x_i^p - x_i\| \le d_{\max}^p, \tag{6}$$

where x_i is the ground-truth position of UAV i; $d_{\max}^p$ is a threshold based on different speeds of targets. The threshold can make UAVs select feasible sampling points in (5) for accurate trajectory prediction. It can also reduce the sensing frequency of targets for real-time tracking imitation.

B. Objective Formulation

The imitation and tracking processes bring additional latency. We can optimize the imitation data size to alleviate the former. The latter can be optimized by exploring suitable tracking paths. The coarse-grained imitation can acquire a DT model based on the positions, velocities, and postures of UAVs and targets as well as physical environment information. Fine-grained imitation can make UAVs exchange mobile information (postures, velocities) of targets with neighbors to perform cooperative trajectory prediction. Both models are simultaneously optimized based on our proposed tiered cooperative tracking algorithm detailed in Section V-B. The flight latency is directly related to the flight energy consumption [22]. The flight energy is $E_i^f = \int_{t-1}^{t} P_i^f(\|v(s)\|) ds$, where $P_i^f(\|v(s)\|)$ is the power with the velocity $v(s)$, where $s \in [t, t+1]$.

Let b_i denote the number of Central Processing Unit (CPU) cycles acquired in unit time for imitation consumption. The total number of CPU cycles is $b_e I_e$. Based on dynamic voltage and frequency scaling technology [23], group leader e can adjust the CPU working frequency $f_{e,u}$ to control the energy consumption, where $f_{e,u} \in (0, f_{e,\max})$, and $f_{e,\max}$ is the maximal CPU frequency. From [24], we know that power consumption is proportional to the cubic frequency:

$$E(I_e) = \sum_{u=1}^{b_e I_e} \kappa_e f_{e,u}^3, \tag{7}$$

where κ_e is the effective capacitance coefficient that depends on the clip characteristic. It is noted that imitation consumption is neglected for the centralized mode with sufficient resources. The system energy consumption is constrained based on the maximal energy budget $E_{\max}$:

$$\sum_{e} (E(I_e) + E_e^f) \le E_{\max}. \tag{8}$$

UAVs and edge servers can dynamically schedule their computing resources to explore the optimal resource allocation solution for tracking imitation and implementation with $E_{\max}$. In this case, the optimization model is formulated as

$$P1: \min \left\{ \lim_{T\to\infty} \frac{1}{T} \sum_{t=0}^{T} \left[\sum_{i=1}^{M} \sum_{k=1}^{K} (t_{i,k}^s + t_i^c + I_i) \right] \right\},$$
$$\text{s.t.} \begin{cases} C1: \ (1), (6), \ (8), \forall e \in \mathcal{E} \\ C2: d_{i,j} \ge d_{\min}, \forall i, j \in \mathcal{M} \\ C3: r_{i,j} \ge r_{\min}, \forall i, j \in \mathcal{M} \end{cases} \tag{9}$$

where $C1$ denotes the constraints of the sensing capability and system energy consumption; $C2$ is the minimal flight distance among UAVs for collision avoidance; $C3$ is the constraint of transmission rates. The objective is to achieve accurate and real-time MTT by optimizing the performance of target sensing, information exchange, and tracking cooperation.

Lemma 1: The P1 is an NP-Hard problem.

Proof: We assume the UAV swarm with M UAVs is decomposed into E groups at time slot t. It is represented as $[\chi_1, \chi_2, \cdots, \chi_E]$ and $\sum_{i=1}^{E} \chi_i = M$. The resource allocation for (8) can be written as $[\psi_1, \psi_2, \cdots, \psi_E]$ and $\sum_{i=1}^{E} \psi_i \le \chi_{\max}$, where ψ_i and χ_E are the available resources of group i and group E, respectively; $\chi_{\max}$ is the maximal budget of available energy. The resource allocation results are infinite theoretically because ψ_i is a real number. The imitation time is undetermined without prior experience. The optimal allocation cannot be obtained in polynomial time.

For cooperative tracking, the association relationship is quantified as a clique problem. We assume UAVs associate all the targets in one group regarded as a graph. The graph has multiple cliques, where each contains u cooperative UAVs and v targets. For a graph with $M+K$ vertices, we need to

explore $\frac{(M+K)!}{(u+v)!(M+K-u-v)!}$ subsets for a suitable clique, which is identified as the classic NP-Hard problem [25]. □

V. Tiered Cooperative Tracking in UAV Swarms

In this section, we present the tiered DT-assisted tracking algorithm to realize low-latency and accurate MTT based on Lemma 1. We decompose the NP-Hard problem into two sub-problems: *coarse-grained MTT imitation* and *fine-grained MTT imitation*.

A. Coarse-Grained MTT Imitation

The proposed coarse-grained MTT imitation block diagram is shown in Fig. 3. Based on the current positions of the UAVs and the targets, our graph learning-based imitation algorithm divides the UAVs into multiple groups to track the targets. The imitation process mainly has five parts: *UAV swarm formation*, *graph operation*, *learning estimation*, *group leader selection*, and *intra-group cooperative tracking*.

1) UAV Swarm Formation: As mentioned in Section III, the adjacency matrix $A = G(V, E)$ representing the associations of UAVs can reflect whether any two UAVs can communicate with each other or not. The information of the targets is used to construct the feature matrix X with $h_{i,j}$. We divide the UAVs into multiple groups for the real-time tracking assignments.

2) Graph Operation: A decomposition result Z_{out} is formulated by a mapping function F:

$$Z_{out} = F(X, A), \tag{10}$$

where the mapping function F can accurately output swarm decomposition results based on position relations among UAVs and targets using the message convolution operation [26]. The UAVs' and targets' information is extracted and represented as X, which is the input of the graph learning network. We use ReLU and SoftMax activation functions to implement graph convention operation for the optimal decomposition result. The result is estimated based on a designed loss function $Loss$. Let $h_i^l \in R^{\dim_l}$ be the hidden representation vector of UAV i with various dimension $\dim_l$. We select all the one-hop neighbors of UAV i to involve the message-passing process as below:

$$h_i^{l+1} = \delta_a \left(W_0^l h_i^l + \sum_{j \in N_i} q_{i,j} {W_1^l}^T h_j^l \right), \tag{11}$$

where δ_a is ReLU function; W_0 and W_1 are weight matrices; N_i is the set of neighbors of UAV i; $q_{i,j} = \frac{1}{\sqrt{D_{i,i} D_{j,j}}}$ is a constant value for normalization, where $D_{i,i}$ and $D_{j,j}$ are the weights of neural layer i and j, respectively. In this case, UAVs can select suitable neighbors to perform cooperative MTT based on computing results from the δ_a. A two-layer graph network is constructed with a singular value decomposition method [27]. The (10) is rewritten as

$$Z_{out} = \text{SoftMax}\left(\widehat{A} \text{ReLU}(\widehat{A} X W_0) W_1 \right), \tag{12}$$

where $\text{SoftMax}(x_i) = \frac{e^{x_i}}{\sum_{c=1}^{C} e^{x_c}}$ where C is the number of classes; $\widehat{A} = \widetilde{D}^{\frac{1}{2}} \widetilde{A} \widetilde{D}^{\frac{1}{2}}$, where $\widetilde{D}$ is the matrix composed of eigenvectors of $\widehat{A}$; $\widetilde{A} = A + I_N$ where I_N is an identity matrix.

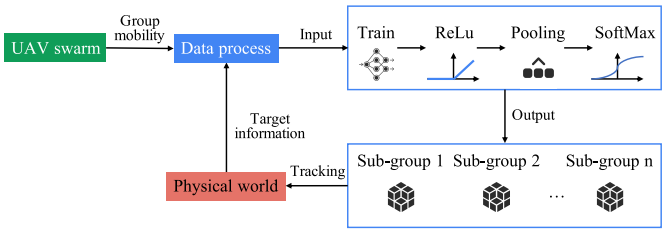

Fig. 3. Block diagram of the proposed coarse-grained MTT Imitation.

Algorithm 1 Coarse-Grained MTT Imitation

Input: Initial position x_t^k, scaling factor κ, sampling weights ω, adjacency matrix A, feature matrix X, weighted matrix W, activation function δ_a.
Output: The optimal decomposition result.

```
Set κ = 0.1
while K ≠ ∅ do
    Predict trajectory of target k based on (6)
while t < T do
    while M ≠ ∅ do
        Initialize feature h_i^0 while each hidden layer l ∈ L do
            h_{N(i)}^l ⟵ ReLU(h_j^{l-1}) Compute h_i^l using (11)
        h_i^l ⟵ h_i^l / ||h_i^l||_2
        Obtain Z_out using (12)
        Compute training loss using (13)
    if target k flies out of the current area and the cloud server is reachable then
        Select UAVs closest to target k for re-decomposition
    else
        if Remote cooperation is required then
            The cloud server adjusts group sensing area
        if the cloud server is unavailable then
            UAVs closing to target k perform distributed re-decomposition
```

3) Learning Estimation: It is challenging to acquire a perfect training dataset in deep learning applications. Therefore, we propose a semi-supervised method to ensure high-efficiency training and learning with the integration of supervised loss function L_1 and unsupervised loss function L_2. The L_1 is represented as $L_1 = -\sum_{l=1}^{L} \sum_{c=1}^{C} \gamma_{l,c} Z_{out}^{l,c}$, where $\gamma_{l,c} = \{0, 1\}$ is an indicator variable. The $L_2 = \sum_{i,j} A_{i,j} \|f(x_i) - f(x_j)\| = f(X)^T L_\Delta f(X)$, where $f(x)$ is a classifier function. The semi-supervised training loss is represented as

$$Loss = L_1 + \lambda L_2, \tag{13}$$

where λ is a hyper-parameter. We can adjust hyper-parameters toward the direction of the minimal loss value. It means we can acquire a satisfied swarm decomposition result.

4) Group Leader Selection: For each UAV group, the cloud will select the group leader flying at the physical center

position of the group in a centralized cooperation mode. If no UAVs are in the center position, the UAV closest to the center position is elected to be the group leader to implement the fine-grained MTT imitation. When the cloud server is unavailable in extreme weather conditions, the UAV swarm can implement a distributed swarm decomposition algorithm based on the above-described *graph operation* and *learning estimation*. The group leaders are elected through information exchange among UAVs. The UAV closest to the center position autonomously announces itself as the leader of other UAVs in the group.

5) Intra-Group Cooperative Tracking: High-speed moving targets can quickly fly out of the current tracking group. It is feasible to re-assign UAVs for tracking the dynamic targets accurately. However, frequent reassignments of the UAVs are time-consuming. To provide an effective reassignment and tracking imitation, we propose a cooperative imitation method with enhanced sensing performance [28] for low-latency tracking. Explicitly, our algorithm enables the cloud server to explore UAVs – close to high-speed moving targets – to implement re-decomposition. The cloud can schedule available computing resources of the UAVs to enable MTT imitation. The imitation result can provide feasible UAV allocation decisions for sequential tracking. Our method can also make these UAVs autonomously perform the distributed re-decomposition for real-time tracking response [29] when the cloud is unreachable. Therefore, our method can effectively schedule the computing resources of UAVs to ensure real-time tracking. The details are represented in Algorithm 1.

B. Fine-Grained MTT Imitation

The group leaders cannot always update UAV information in real time due to undetermined latency on sensing and transmission between the physical and virtual worlds. We deploy the same number of UAVs as in the physical world to explore accurate imitation in the virtual world. In the centralized mode, the group leaders distribute the imitation results to UAVs. While in the distributed mode, UAVs can independently train DT models to acquire the MTT results. We design a universal algorithm architecture as shown in Fig. 4, where UAVs can train and estimate the target information based on the Multi-Agent Deep Deterministic Policy Gradient (MADDPG) architecture. It includes a critic module and an actor module. Each module supports a policy network and an estimation network. UAVs can learn tracking actions based on the local information S_i. All the actions $A = \{A_1, \cdots, A_M\}$ of UAVs are estimated centrally. The policy network trains the data based on constructed *state space* S_i. The tracking action from *action space* A_i is obtained with the aid of actions of other UAVs. Meanwhile, the estimation network evaluates the tracking performance with an estimation function. The imitation process is quantified as a Stochastic Game (SG) problem with a tuple $\{S_i, A_i, \mathcal{T}, R_i\}$, where $\mathcal{T}$ is a transfer function and R_i is a reward function to estimate the action.

The UAV tracking paths are included in the reward to ensure low-latency tracking. To ensure cooperative MTT, we propose a *reaction-diffusion scheme* in the fine-grained MTT imitation. The diffusion concentration positively relates to the targets' speeds estimated by historical tracking experiences and trajectory prediction results. The scheme is enabled with the MADDPG architecture for accurate tracking. The diffusion can guide the suitable UAVs to perform sequential MTT in each group. The state space S_i is divided into four parts:

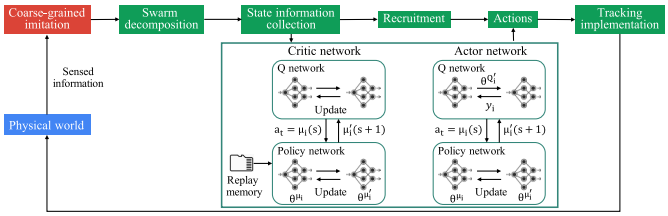

Fig. 4. Block diagram of the fine-grained MTT Imitation.

1) States of UAV i: $s_i = \{a_i, v_i, p_i, \varrho_i, \{d_{i,k}\}\}$, where a_i, v_i, and p_i are found from h_i; ϱ_i is the height of UAV i; $\{d_{i,k}\}$ is the set of physical distances between UAV i and target k.
2) States of one-hop neighbors: $o_i = \{\{d_{i,j}\}, h_j\}$, where $\{d_{i,j}\}$ is the set of physical distance between UAV i and its one-hop neighboring UAVs; h_j is feature information of UAV j.
3) States of targets: $h_{i,k}$, where $h_{i,k}$ is the feature information of target k sensed by UAV i.
4) Environmental states: $l_i = \{G_t, B_t\}$, where G_t and B_t are noise and terrain information.

The action space is $A_i = \{X_i, \kappa_i, \{\kappa_{i,j}\}, \theta_i\}$, where X_i is the flight status of UAV i including position and pitch angle; $\kappa_i \in [0, 1]$ is a parameter to adjust the diffusion concentration value; $\{\kappa_{i,j}\}$ is the set of UAVs receiving the diffusion information of UAV i from j; θ_i is the updated concentration. The initial concentration is $\theta_i = \kappa_i J_k^d$, where J_k^d is the unit locomotion of target k. As shown in Fig. 5, when UAV j receives the diffusion information of UAV i, the target attribute is added to its state space. UAVs can update the current actions to adjust their sensing directions when recruited successfully. In this case, UAVs can promote sensing efficiency to guarantee a high successful tracking ratio. The diffusion will continue with updated concentration until recruiting suitable numbers of cooperators:

$$\theta_i = \begin{cases} \theta_i \times \alpha_i, & \theta_i \text{ is selected}, \\ \theta_i + \beta_i, & \theta_i < \gamma_{\max}, \\ 0, & \text{otherwise}, \end{cases} \tag{14}$$

where α_i and β_i belong to [0,1]; $\gamma_{\max}$ is the maximal concentration. The R_i is redefined as

$$\begin{aligned} &R_i(S_i, A_i) \\ &= r_i(S_i, A_i) + \frac{\alpha_i}{E_e} \sum_{k \neq E_e} \max\left(r_j^t(S_j, A_j) - r_i^t(S_i, A_i), 0\right) \\ &\quad + \frac{\beta_i}{E_e} \sum_{k \neq E_e} \max\left(r_i^t(S_i, A_i) - r_j^t(S_j, A_j), 0\right), \end{aligned} \tag{15}$$

where E_e is the number of targets in group e; $r_i(S_i, A_i) = \frac{1}{E_e} \sum_{k=1}^{E_e} [\Delta D_{j,k} + \Delta D_{i,k}]$, and $\Delta[f] = f(t-1) - f(t)$; α_i and β_i can be set as 5 and 0.05 [30], respectively. Based on this, UAVs can learn a feasible action from the policy network. The state and action are cached to the replay memory Ω. The

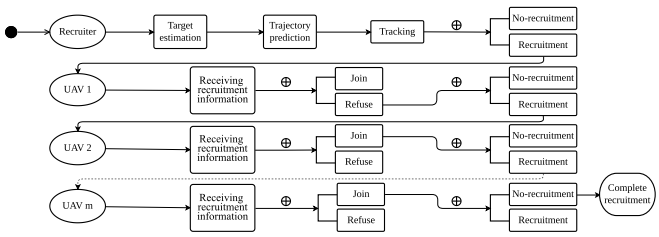

Fig. 5. Flow chart of recruitment-based cooperative tracking.

actions are evaluated based on the Bellman equation:

$$L(\theta^Q) = E_{S,A,R,S'}\left[\frac{1}{M}\sum_i \left(Q^\mu(S_i,(A_1,\cdots,A_M)) - Z\right)^2\right], \tag{16}$$

where S' is the next state; $Z = R_i + \gamma Q^{\mu'}(S_i, A_i)|_{A_i'=\mu_i'(S_i)}$ where γ is the discount factor; θ^Q is a hyper-parameter of estimation network. We can minimize the $L(\theta^Q)$ to make UAVs perform satisfying tracking actions with the aid of actions of other UAVs. We can explore the optimal loss value based on the policy gradient $J(\theta^\mu)$ which is given by

$$\begin{aligned}&\nabla_{\theta^\mu} J(\theta^\mu)\\ &= E_{S,A\backsim\Omega}\Big[\frac{1}{M}\\ &\quad\sum_i \nabla_{\theta^\mu}\mu(A_i|S_i)\nabla_{A_i}Q^\mu(S_i,(A_1,\cdots,A_M))|_{A_i=\mu(S_i)}\Big].\end{aligned} \tag{17}$$

Based on the chain rule [31], the parameters of neural network are updated by

$$\begin{aligned}\nabla_{\theta^C} J(\theta^C) = E_{S,A\backsim\Omega}\Big[&\sum_i w_i(C_i)\nabla_{C_i}\mu(A_i|C_i)\nabla_{C_i}\mu(A_i|C_i)\\ &\nabla_{A_i}Q^\mu(S_i,A_i)|_{A_i=\mu(S_i)}\Big],\end{aligned} \tag{18}$$

where $w_i(\cdot)$ denotes the cooperators of UAV i; θ^C is a hyper-parameter of policy network. The parameters are updated as $\theta' = \tau\theta + (1-\tau)\theta'$. The action is optimized as

$$\begin{aligned}L(\theta^a) = &-\Delta\hat{Q}_i \log\Big(p(C_i|\theta^a)\Big)\\ &-(1-\hat{Q}_i)\log\Big(1-p(C_i|\theta^a)\Big).\end{aligned} \tag{19}$$

UAVs can perform cooperative tracking by minimizing the $L(\theta^a)$ value. The details are presented in Algorithm 2. The tiered DT tracking is shown in Fig. 6 with the switch of the coarse-grained and fine-grained imitations. For the coarse-grained imitation, the reachable cloud can implement swarm decomposition operation based on the position information of UAVs and targets. When the cloud is unreachable, UAVs can autonomously explore suitable cooperators for the decomposition operation. The coarse-grained imitation results can make the subgroups associate appropriate targets for accurate tracking. It can also manage subgroups to perform cooperative tracking through a low-latency re-decomposition manner among partial subgroups instead of all of them. In each subgroup, a group leader elected by members implements the fine-grained imitation based on MADDPG architecture with

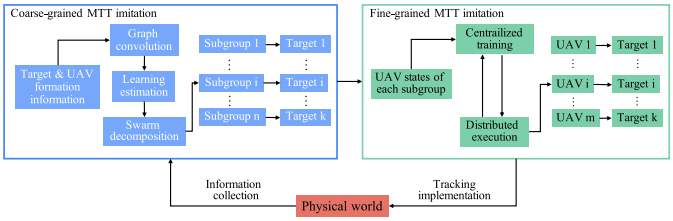

Fig. 6. Illustration of tiered DT-assisted tracking imitation.

Algorithm 2 Fine-Grained MTT Imitation

Input: Observation information S; MADDPG network parameters θ^Q, θ^μ; updated weighted γ; Neural network parameters θ^C and θ^a; replay memory Ω; κ_i; the set of recruited UAVs U.

Output: The cooperative tracking decision.

Definition: $\gamma = 0.99$.

Obtain the number of UAVs of group e
while *each episode in all rounds* **do**
  Set an initial action μ and receive the relevant state
  Construct tracking environment
while $t < T$ **do**
  swarm decomposition using Algorithm 1
  while $\mathcal{E} \neq \varnothing$ **do**
    $a_{i,t} \longleftarrow \mu_{\theta_i}(S_{i,t}) + N_t$
  if *UAV i acquire cooperation and UAV j selects θ_i* **then**
    $U \longleftarrow U \cup j$
  Update concentration θ_i by (14)
  Store the experience to Ω, and evaluate the action using the estimation network
  Compute the reward using (15), Q-value using (17), and loss gradients using (16)
  Update the gradient using (18) and optimize the action using (19)

centralized training and distributed execution. The imitation decisions can make UAVs perform sequential tracking for a high successful tracking ratio.

Lemma 2: Algorithm 2 converges synchronously.

Proof: We start the proof based on the action-value function in (16) which forms a contraction mapping with the convergent point Q^* under the following assumptions.

Assumption 1: The action value is visited infinitely. The reward is limited by a constant P.

Assumption 2: In the SG process, agents can obtain the equilibrium policy $\pi^* = \{\pi_1^*, \pi_2^*, \cdots, \pi_M^*\}$ based on the greedy iteration in the following cases:

1) The global optimization holds: $E_{\pi^*}[Q_i^\mu(S)] \geq E_\pi[Q_i^\mu(S)], \forall\pi$;
2) A saddle point is obtained: $E_{\pi^*}[Q_i^\mu(S)] \geq E_{\pi_i}E_{\pi_{-i}^*}[Q_i^\mu(S)]$ and $E_{\pi^*}[Q_i^\mu(S)] \geq E_{\pi_i}{*}E_{\pi_{-i}}[Q_i^\mu(S)]$.

Based on the above assumptions, the SG process H_t with a tuple $\{S_i, A_i, \mathcal{T}, R_i\}$ defined as

$$H_{t+1}(x) = (1-\alpha_t(x))H_t(x) + \alpha_t(x)F_t(x) \tag{20}$$

can converge to zero with probability 1, if

1) $0 \leq \alpha_t(x) \leq 1$, $\sum_t \alpha_t(x) = \infty$, and $\sum_t \alpha_t^2 \leq \infty$;
2) $x \in \sum_i S_i$ and $\sum_i S_i \leq \infty$;
3) $\|E[F_t(x)]|\mathbf{F}_t\|_d \leq \gamma \|H_t\|_d + z_t$, where $\gamma \in [0, 1)$, and z_t can converge to 0;
4) $\mu[F_t(x)|\mathbf{F}_t] \leq K(1 + \|H_t\|_d^2)$ with $K \geq 0$, where $\|*\|_d$ is a weighted maximum norm.

The first and second conditions are satisfied. The third and fourth conditions are proved using the Q-function formulated in Section V and (20). The H_t and F_t are rewritten as

$$H_t(S_t, A_t) = Q_t(S_t, A_t) - Q^*(S_t, A_t), \tag{21}$$

$$F_t(S_t, A_t) = R_t + \gamma Q^{\mu}(S_{t+1}) - Q^*(S_t, A_t). \tag{22}$$

Based on (22), the third condition holds because

$$\begin{aligned} F_t(S_t, A_t) &= R_t + \gamma Q^{\mu}(S_{t+1}) - Q^*(S_t, A_t) \\ &= R_t + \gamma Q^{\mu*} - Q^*(S_t, A_t) \\ &\quad + \gamma \left[Q^{\mu}(S_{t+1}) - Q^{\mu*}(S_t, A_t)\right] \\ &= R_t + \gamma Q^{\mu*}(S_{t+1}) - Q^*(S_t, A_t) + c_t(S_t, A_t) \\ &= F_t^*(S_t, A_t) + c_t(S_t, A_t). \end{aligned} \tag{23}$$

With *Assumption 2*, we can derive that $c_t(S_t, A_t) = \gamma \left[Q^{\mu}(S_{t+1}) - Q^{\mu*}(S_t, A_t)\right]$ converges since all the agents share the same globally or partially optimal equilibrium policies. Therefore, Q^{μ} can asymptotically converge to $Q^{\mu*}$. For the fourth condition, we can derive the following result based on contraction mapping theory [32]:

$$\begin{aligned} \mu[F_t(S_t, A_t)|\mathbf{F}_t] &= E\left[(R_t + \gamma Q^{\mu}(S_{t+1}) - Q^*(S_t, A_t))^2\right] \\ &= E\Big[(R_t + \gamma Q^{\mu}(S_{t+1}) - \sum_{S_i, A_i} Q^*)^2\Big] \\ &= \mu\left[R_t + \gamma Q^{\mu}(S_{t+1})|\mathbf{F}\right] \leq K(1 + \|H_t\|_d^2). \end{aligned} \tag{24}$$

All the conditions are met to make H_t converge to 0, namely Q^{μ} converges to Q^*. Consequently, algorithm 2 converges. □

C. Algorithm Complexity Analysis

We analyze the complexity of our tiered DT-assisted MTT system in two parts: **coarse-grained imitation** and **fine-grained imitation**. For the coarse-grained imitation, we use a graph convolution algorithm to support the coarse-grained UAV swarm decomposition for tracking in real time. In this case, the time complexity of the swarm decomposition is $O(L \cdot N \cdot F^2)$ [33], where L is the layer number of the neural network; N is the number of the eigenvalues of $\hat{A}$; F is the number of feature elements of h_i. With a two-layer graph network, the time complexity for the coarse-grained imitation is $O(2 \cdot N \cdot F^2)$. The resource allocation is in polynomial time with $O(1)$ for the fine-grained imitation. The time complexity of the primary network falls on the matrix inversion operation with $O(k(\theta))$, where $k(\theta)$ is a function whose input θ is the number of hidden layers. The overall complexity of our proposed algorithm is $O(2 \cdot N \cdot F^2 \cdot k(\theta))$. The time is lower than traditional deep reinforcement learning because we divide the UAV swarm into multiple groups based on tiered MTT instead of all UAVs with a single-layer MTT operation.

TABLE II
SIMULATION PARAMETERS

Parameter description	Value
Number of mobile targets	[30, 80]
Average moving speed of the UAVs	56 km/h
Moving speed of the targets	[32 km/h, 90 km/h]
MTT tracking area	3000 m × 3000 m
Pitch angle of the UAVs	$[-130°, +40°]$
Angular-rate of horizontal rotation	$[-100°, +100°]$
The scale factor of Unscented Filter κ	0.1
Minimal safe flight distance of the UAVs	3 m
Transmission power of UAVs	[60 mW, 100 mW]
Communication bandwidth	[50 MHz, 100 MHz]
Average sensing rate of the UAVs	1 MByte/s
Horizontal sensing distance of the UAVs	30 m
Gaussian White Noise	-96 dBm/Hz
Acceptable maximal system latency	2 seconds

VI. PERFORMANCE EVALUATION

In this section, we evaluate the performance of our proposed tiered MTT. The sensing of the targets in the simulation is based on the actual image and UWB data collected by commercial UAVs. The fine-grained imitation is implemented at the selected leaders in each group with an onboard computing Manifold [34]. The coarse-grained imitation is executed in non-leader UAVs, which are also equipped with the Manifold. We use Python to implement the proposed algorithm based on Pytorch architecture [35]. We record and represent the tracking process in NS-3 using C++. The performance of our proposed algorithm is evaluated under different numbers of UAVs and mobile targets. The main simulation parameters are summarized in Table II.

We compare the performance of our tiered MTT with the following five benchmarks:

1) *Fuzzy logic-based target tracking* [36]: The fuzzy logic scheme is leveraged to estimate the priority of tracked targets based on a given rule. It is integrated into the genetic algorithm to improve target detection accuracy.
2) *Conventional DDPG* [37]: Each UAV runs a DDPG architecture to learn a suitable tracking decision based on the sensed information.
3) *Non-cooperative tracking*: It leverages the same MA-DDPG architecture to implement the multi-grained MTT imitation. However, the scheme cannot enable UAVs to recruit cooperators for real-time tracking without the proposed reaction-diffusion method.
4) *Evolution theory-based multiple targets tracking* [38]: It utilizes an adaptive differential evolution scheme to predict trajectories of targets for accurate tracking cooperatively.
5) *Multi-Agent Reinforcement Learning-based Target Tracking (MARL)* [39]: UAVs learn suitable tracking actions with a centralized training and distributed execution pattern.

A. Preliminary Evaluation

We randomly fly the targets in an area of interest in our UESTC campus based on the DJI Pilot APP. The targets' flight paths are recorded in UAVs. The information includes

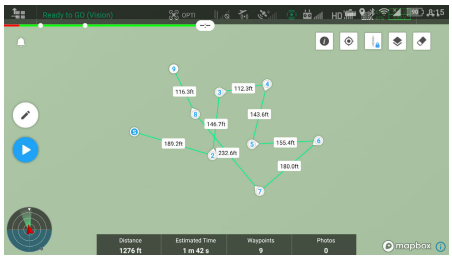

Fig. 7. Target trajectory planning.

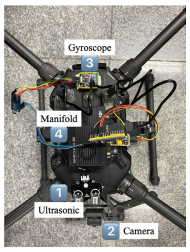

Fig. 8. UAV with sensors.

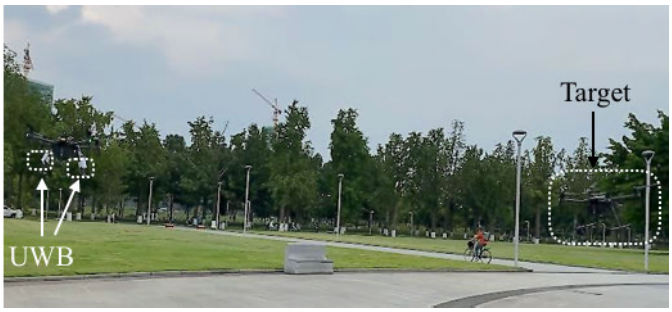

Fig. 9. Target detection using UWB.

the velocities of targets and physical distances between UAVs and targets sensed by the UWB sensor, the captured target image by the onboard camera, and the positions of the UAVs obtained from GPS.

Different target trajectories are leveraged to evaluate the robustness and effectiveness of our proposed algorithm. The target trajectories are randomly planned using DJI Pilot APP shown in Fig. 7. GPS information is transferred to a Cartesian coordinate using the seven-parameter transformation method. In Fig. 8, vision cameras recognize the shapes of targets based on YOLOv5 [40]. UWB sensors obtain the relative physical distances among the UAVs and the targets and position information of the targets [41]. We can ensure accurate tracking by frequently enabling target detection operations using the UWB sensor. It causes significant consumption of sensing and computing resources. We can implement trajectory prediction using the formulated model (5) to alleviate the highly frequent target sensing. However, it is difficult to perform accurate predictions of random target trajectories in the long-term tracking process due to the accumulation of prediction errors. Fortunately, our prediction model (5) can provide accurate prediction results for short-range random moving trajectories by simulating the random distribution based on a sampling method [21]. In this case, to trade off the frequent target detection and accurate tracking, we enable UAVs to implement trajectory prediction using the model (5) in the following one fixed motion time slot T based on the current target detection result. At the time T, we can use the UWB sensor

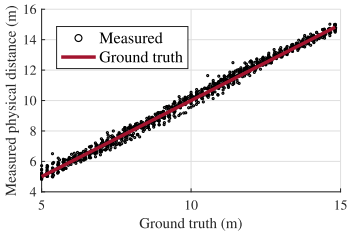

Fig. 10. UWB-measured distances.

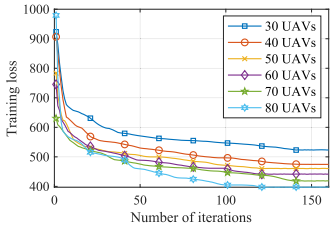

Fig. 11. Swarm decomposition.

to optimize the prediction result of the random motion model. The way can eliminate the accumulated prediction error to perform accurate trajectory prediction in lone-term tracking process. Based on this, UAVs can accurately track randomly moving targets without frequent target detection. Weather conditions are obtained by temperature and humidity sensors. We acquire multiple sets of physical distance data among UAVs and targets based on UWB sensors in Fig. 9. The test results scatter around the ground truth (i.e., the actual physical distance) closely, as shown in Fig. 10. It is because that UAVs' postures change dynamically during the tracking process. We use median values as test results to evaluate the accuracy and real-time of MTT.

B. Evaluation of Coarse-Grained Imitation

When the cloud server is available, it can decompose UAVs into multiple groups based on h_i and $h_{i,j}$. Furthermore, UAVs can autonomously decompose based on our algorithm in Section V-A when the cloud server is unavailable. We use NS-3 to imitate the swarm decomposition for optimal target association. Fig. 11 depicts the swarm performance of our coarse-grained tracking imitation method. All the tracking scenarios with different numbers of mobile targets realize learning convergence with stable performance. The convergence performance improves with the increase in the number of targets because implementing the deep learning algorithm requires a large training data size. The specific decomposition process is represented in Fig. 12.

We present the decomposition results with different targets to estimate the coarse-grained imitation performance. Fig. 12(a) depicts the swarm decomposition with 20 UAVs and 40 targets. Our algorithm decomposes the UAV swarm into four groups, each marked with different colors. We use different shapes and labels to mark UAVs and targets. The UAV is marked as a circle with the label "U". The target is signed as a triangle with the label "T". Based on their geographic position information, our algorithm can always allocate feasible UAVs to associate targets moving in different locations. The ratio of the number of UAVs to the number of targets is approximately equal for different sub-groups. UAVs can effectively schedule

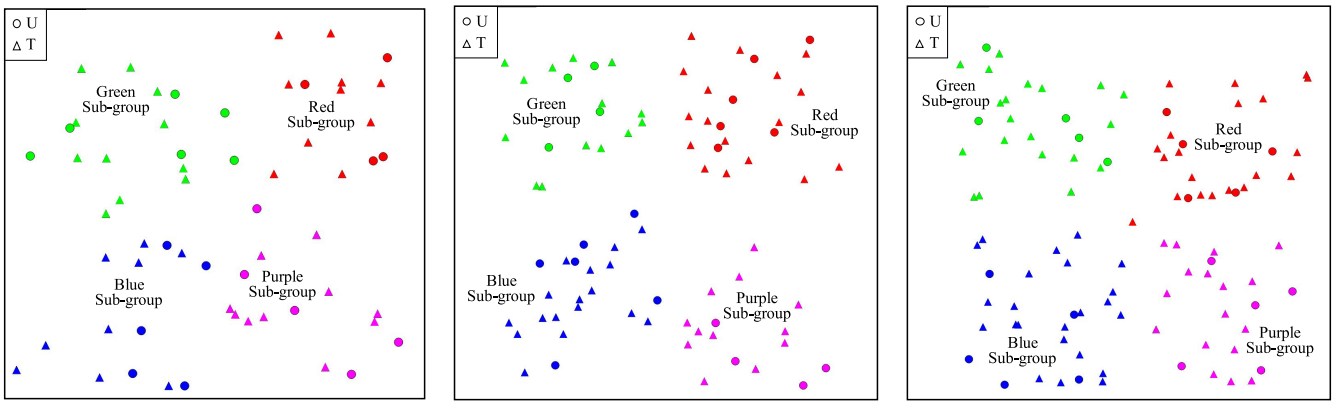

(a) 40 mobile targets (b) 60 mobile targets (c) 80 mobile targets

Fig. 12. The swarm decomposition results under 20 UAVs.

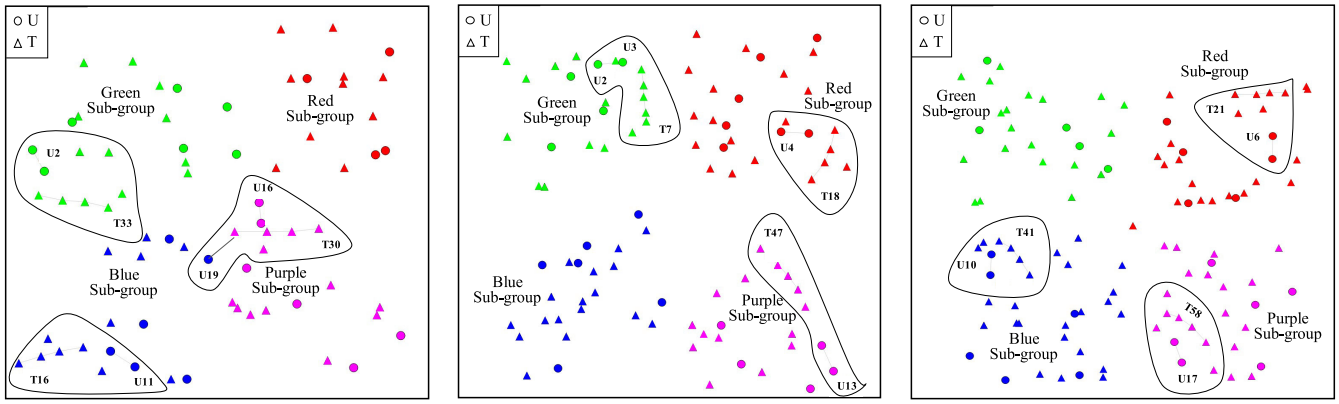

(a) 40 mobile targets (b) 60 mobile targets (c) 80 mobile targets

Fig. 13. The transient state of swarm cooperation under 20 UAVs.

their computing resources for low-latency imitation using our cooperative imitation method. The imitation results can ensure accurate tracking and provide optimal computing resources for each sub-group for the fine-grained imitation. The result of 20 UAVs tracking 60 targets is given in Fig. 12(b). We can discover that UAVs can sense suitable targets. UAVs cannot continue to implement the tracking operation when targets escape from the detection area. Our algorithm still achieves the optimal associations when the number of targets increases. Fig. 12(c) shows the decomposition result with 20 UAVs and 80 targets. Our algorithm always explores and obtains the optimal decomposition result. Our algorithm achieves high robustness and stability as the number of targets increases.

C. Evaluation of Fine-Grained Imitation

The coarse-grained tracking imitation re-decomposes UAV swarms to track high-speed moving targets in real time. However, ensuring inter-group tracking cooperation with collision avoidance among UAVs is necessary. We present the inter-group tracking cooperation performance in Fig. 13 with diverse targets. We simulate the tracking process using the NS3 simulation tool with 20 UAVs and 40 targets in Fig. 13(a). We find that the UAV U11 can accurately observe multiple targets, and meanwhile, can cooperatively track the T16. Our fine-grained imitation method can assist UAVs in acquiring mobile trajectories of targets to dynamically associate feasible targets. UAVs can cooperatively predict the trajectories of targets by exchanging the trajectory information with neighbors for intra-group tracking cooperation with a high successful tracking ratio. In addition, UAVs can share lightweight prediction results with neighbors to cooperatively plan tracking paths for real-time tracking. In this case, UAVs can also dynamically associate optimal targets to further enhance the cooperative intra-group tracking capability.

The case of 20 UAVs tracking 60 targets is shown in Fig. 13(b). The U2 and U3 track T7 – which moves at high speed within the detection area – cooperatively at different slots. The system's robustness is verified by tracking diverse targets with random velocities. Our reaction-diffusion scheme is effective in guaranteeing inter-group cooperation. In a more complex MTT system with 20 UAVs and 80 targets, as shown in Fig. 13(c), these targets can also be accurately sensed and tracked by the UAVs with a high successful tracking ratio. We find that different UAVs can continuously track targets at various speeds. The qualitative analysis shows that our system is robust under the scenarios of other numbers of targets with multiple velocities.

D. System Evaluation

We continue to present the evaluation of the whole system shown in Fig. 14(a). Under 20 UAVs, all the rewards gradually increase to a stable status with 500 tests. In addition, the highest reward is obtained in the scenario of 80 targets with sufficient target information. All the convergence times

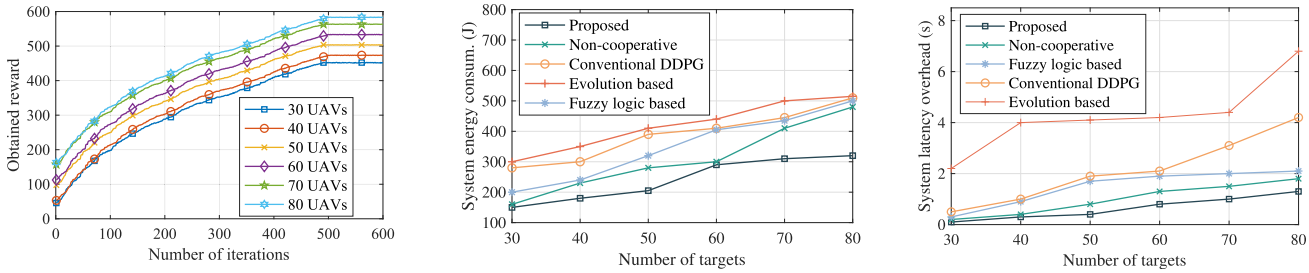

(a) Rewards vs. number of iteration (b) Energy consum. vs. number of targets (c) Latency vs. number of targets

Fig. 14. The multi-dimensional comparisons under 20 UAVs and different number of targets.

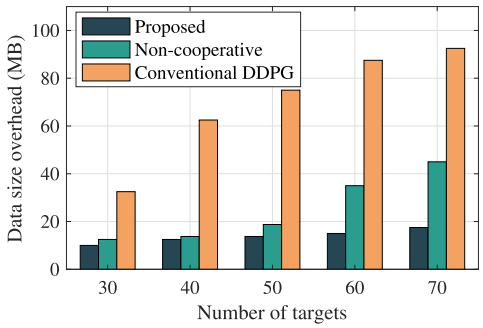

Fig. 15. Data size overhead vs. number of targets.

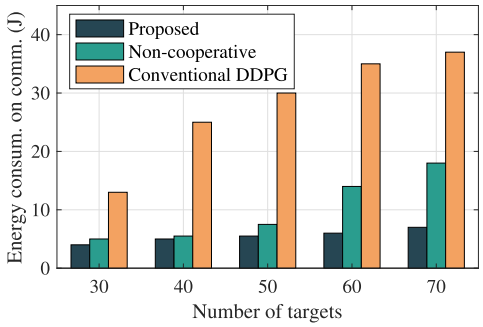

Fig. 16. Energy consumption vs. number of targets.

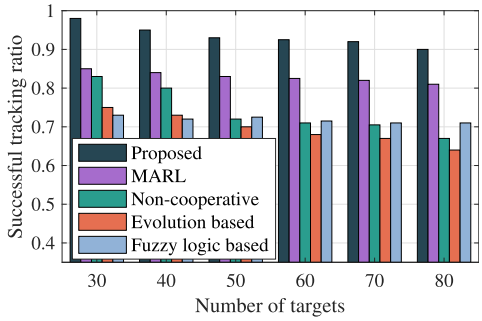

Fig. 17. Success tracking ratio vs. number of targets.

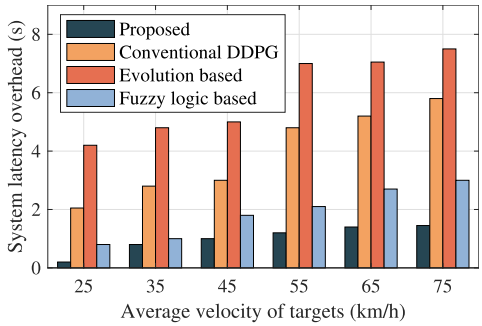

Fig. 18. System latency vs. number of targets.

are acceptable under an average of 500 iterations. UAVs can explore optimal paths to perform tracking cooperation. It is verified in Fig. 14(b) by being compared to the benchmarks. Our algorithm realizes low-energy tracking using the same system parameters as in the benchmarks. The evolution theory-based algorithm consumes the maximal energy consumption. It is because multiple UAVs may track the same target simultaneously with heuristic characteristics. Compared to the non-cooperative, fuzzy logic-based, and conventional DDPG algorithms, our algorithm reduces the system energy consumption by 33.3%, 52.3%, and 64.3%, respectively.

Fig. 14(c) shows the system latency under 20 UAVs. The system latency increases gradually with the number of targets for all the benchmarks. It is time-consuming to track incremental targets. Nonetheless, the speed of increase for the system latency is the lowest in our algorithm. This is because our multi-grained imitation method decouples the heavy tracking missions based on the difference of resources among the UAVs, the edge, and the cloud. We can achieve low-latency tracking for diverse numbers of targets. Besides, our MTT system is stable under various velocities of targets. It validates that our tiered DT can enhance tracking efficiency. The evolution theory-based algorithm has the highest latency due to frequent trial and error operations. Our system reduces the system latency by 38.5%, 66.7%, 75.0%, and 80.9% on average, compared to non-cooperative, fuzzy logic-based, conventional DDPG, and evolution-based algorithms.

Fig. 15 and Fig. 16 compare communication overhead with data size overhead and energy consumption on communication under different numbers of targets. Our solution can reduce the communication data size and energy consumption compared to the conventional DDPG algorithm and the non-cooperative algorithm. It is because cooperative imitation can assist UAVs in finding feasible cooperators accurately based on the tiered DT framework. The proposed reaction-diffusion mechanism can effectively reduce the extra data size and the energy consumption on communication. It can enable UAVs to exchange information with partial neighbors instead of all the UAVs. Our solution reduces the energy consumption on communication by 25.0% and 76.9%, compared to the non-cooperative and the DDPG algorithm, respectively.

The successful tracking ratio $\jmath$ is defined from (1):$\jmath = \lim_{T\to\infty} \frac{1}{T}\sum_{t=0}^{T} \frac{\sum_{i=1}^{M}\sum_{k=1}^{K} P_{i,k}}{MK}$. The comparison is shown in Fig. 17 under different numbers of targets. Our algorithm maintains a successful tracking ratio of over 90% under

different tracking scenarios. In theory, 20 UAVs can cooperatively sense up to 153 mobile targets while maintaining a 75% successful tracking ratio. The fuzzy logic-based algorithm reduces the successful tracking ratio when the number of targets increases. The logic-based algorithm is based on a pre-designed matching rule, making it unsuitable for the dynamic MTT. Our tiered DT can effectively observe multiple targets with high speeds to implement accurate MTT based on multi-grained cooperative imitation. The imitation can ensure a high successful tracking ratio with low imitation latency. Meanwhile, the high system stability is maintained to extend to large-scale tracking applications with overloaded targets. Compared to the MARL, non-cooperative, and evolution theory-based algorithms, ours improves the successful tracking ratio by 15.4%, 26.7%, and 30.1%, respectively.

The moving speeds of the targets can also affect the tracking performance. The MTT system is expected to ensure low-latency overhead with deep swarm cooperation. Fig. 18 depicts the comparison between system latency and velocities of the mobile targets. Based on the average speed of UAVs at 56 km/h, the whole latency increases with the velocities of the targets for all the algorithms. Nonetheless, our algorithm holds the lowest latency overhead under 1.5s. The response latency is acceptable based on the parameters in Table II. The evolution theory-based algorithm performs worst with high exploration time, especially in complicated MTT scenarios. Our algorithm, on average, can reduce 50.0%, 74.1%, and 79.4% of the latency, respectively, compared to the fuzzy logic-based, conventional DDPG, and evolution-based algorithms.

VII. Conclusion

We design a tiered DT-assisted tracking framework to ensure accurate and real-time MTT. To improve tracking performance of UAV swarm, we propose a multi-grained cooperative MTT system for real-time tracking response. We propose a cooperative tracking algorithm to ensure a high successful tracking ratio by coordinating remote UAVs for sequential tracking. The results demonstrate that our proposed algorithm reduces tracking energy consumption with optimal tracking paths for high-efficiency MTT. There still exist technical challenges of DT for imitating higher-speed moving targets in real time based on our tiered DT framework. In the future, we will deeply explore the integration of the physical world and the virtual world with the multi-tiered imitation pattern for a more effective MTT.

References

[1] M. Liwang, Z. Gao, and X. Wang, "Let's trade in the future! A futures-enabled fast resource trading mechanism in edge computing-assisted UAV networks," *IEEE J. Sel. Areas Commun.*, vol. 39, no. 11, pp. 3252–3270, Nov. 2021.

[2] M. Gapeyenko, D. Moltchanov, S. Andreev, and R. W. Heath Jr., "Line-of-sight probability for mmWave-based UAV communications in 3D urban grid deployments," *IEEE Trans. Wireless Commun.*, vol. 20, no. 10, pp. 6566–6579, Oct. 2021.

[3] W. Sun, G. Tang, and K. Hauser, "Fast UAV trajectory optimization using bilevel optimization with analytical gradients," *IEEE Trans. Robot.*, vol. 37, no. 6, pp. 2010–2024, Dec. 2021.

[4] X. Chen, S. Leng, J. He, and L. Zhou, "Deep-learning-based intelligent intervehicle distance control for 6G-enabled cooperative autonomous driving," *IEEE Internet Things J.*, vol. 8, no. 20, pp. 15180–15190, Oct. 2021.

[5] K. Xiong, S. Leng, C. Huang, C. Yuen, and Y. L. Guan, "Intelligent task offloading for heterogeneous V2X communications," *IEEE Trans. Intell. Transp. Syst.*, vol. 22, no. 4, pp. 2226–2238, Apr. 2021.

[6] J. Du, C. Jiang, J. Wang, Y. Ren, and M. Debbah, "Machine learning for 6G wireless networks: Carrying forward enhanced bandwidth, massive access, and ultrareliable/low-latency service," *IEEE Veh. Technol. Mag.*, vol. 15, no. 4, pp. 122–134, Dec. 2020.

[7] Y. Zhu, M. Mallick, S. Liang, and J. Yan, "Generalized labeled multi-Bernoulli multi-target tracking with Doppler-only measurements," *Remote Sens.*, vol. 14, no. 13, p. 3131, Jun. 2022. [Online]. Available: https://www.mdpi.com/2072-4292/14/13/3131

[8] Z. Lin et al., "DRESIA: Deep reinforcement learning-enabled gray box approach for large-scale dynamic cyber-twin system simulation," *IEEE Open J. Comput. Soc.*, vol. 2, pp. 321–333, 2021.

[9] X. Hu, Y. Liu, and G. Wang, "Optimal search for moving targets with sensing capabilities using multiple UAVs," *J. Syst. Eng. Electron.*, vol. 28, no. 3, pp. 526–535, Jun. 2017.

[10] L. Paull, C. Thibault, A. Nagaty, M. Seto, and H. Li, "Sensor-driven area coverage for an autonomous fixed-wing unmanned aerial vehicle," *IEEE Trans. Cybern.*, vol. 44, no. 9, pp. 1605–1618, Sep. 2014.

[11] Y. Li et al., "Data collection maximization in IoT-sensor networks via an energy-constrained UAV," *IEEE Trans. Mobile Comput.*, vol. 22, no. 1, pp. 159–174, Jan. 2023.

[12] F. Y. P. Feng, M. Rihan, and L. Huang, "Positional perturbations analysis for micro-UAV array with relative position-based formation," *IEEE Commun. Lett.*, vol. 25, no. 9, pp. 2918–2922, Sep. 2021.

[13] J. Yoon, A.-H. Lee, and H. Lee, "Rendezvous: Opportunistic data delivery to mobile users by UAVs through target trajectory prediction," *IEEE Trans. Veh. Technol.*, vol. 69, no. 2, pp. 2230–2245, Feb. 2020.

[14] X. Huang, J. Liang, X. Shen, and Q. Liang, "A multimodal data harness approach of mobile sensors trajectory planning for target tracking," *IEEE Internet Things J.*, vol. 10, no. 11, pp. 9252–9261, Jun. 2023.

[15] Z. Yang, J. Du, Z. Xia, C. Jiang, A. Benslimane, and Y. Ren, "Secure and cooperative target tracking via AUV swarm: A reinforcement learning approach," in *Proc. IEEE Global Commun. Conf. (GLOBECOM)*, Dec. 2021, pp. 1–6.

[16] J. Du, B. Jiang, C. Jiang, Y. Shi, and Z. Han, "Gradient and channel aware dynamic scheduling for over-the-air computation in federated edge learning systems," *IEEE J. Sel. Areas Commun.*, vol. 41, no. 4, pp. 1035–1050, Apr. 2023.

[17] K. Meng, D. Li, X. He, and M. Liu, "Space pruning based time minimization in delay constrained multi-task UAV-based sensing," *IEEE Trans. Veh. Technol.*, vol. 70, no. 3, pp. 2836–2849, Mar. 2021.

[18] W. Feng et al., "Hybrid beamforming design and resource allocation for UAV-aided wireless-powered mobile edge computing networks with NOMA," *IEEE J. Sel. Areas Commun.*, vol. 39, no. 11, pp. 3271–3286, Nov. 2021.

[19] J. G. Andrews, T. Bai, M. N. Kulkarni, A. Alkhateeb, A. K. Gupta, and R. W. Heath Jr., "Modeling and analyzing millimeter wave cellular systems," *IEEE Trans. Commun.*, vol. 65, no. 1, pp. 403–430, Jan. 2017.

[20] F. Scarselli, M. Gori, A. C. Tsoi, M. Hagenbuchner, and G. Monfardini, "The graph neural network model," *IEEE Trans. Neural Netw.*, vol. 20, no. 1, pp. 61–80, Jan. 2009.

[21] S. Julier, J. Uhlmann, and H. F. Durrant-Whyte, "A new method for the nonlinear transformation of means and covariances in filters and estimators," *IEEE Trans. Autom. Control*, vol. 45, no. 3, pp. 477–482, Mar. 2000.

[22] K. Wang, J. Li, Y. Yang, W. Chen, and L. Hanzo, "Content-centric heterogeneous fog networks relying on energy efficiency optimization," *IEEE Trans. Veh. Technol.*, vol. 69, no. 11, pp. 13579–13592, Nov. 2020.

[23] Y. Mao, C. You, J. Zhang, K. Huang, and K. B. Letaief, "A survey on mobile edge computing: The communication perspective," *IEEE Commun. Surveys Tuts.*, vol. 19, no. 4, pp. 2322–2358, 4th Quart., 2017.

[24] J. M. Kim, Y. G. Kim, and S. W. Chung, "Stabilizing CPU frequency and voltage for temperature-aware DVFS in mobile devices," *IEEE Trans. Comput.*, vol. 64, no. 1, pp. 286–292, Jan. 2015.

[25] R. M. Karp, "Reducibility among combinatorial problems," in *Complexity of Computer Computations*. Boston, MA, USA: Springer, 1972, pp. 85–103.

[26] K. Guo, Y. Hu, Z. Qian, Y. Sun, J. Gao, and B. Yin, "Dynamic graph convolution network for traffic forecasting based on latent network of Laplace matrix estimation," *IEEE Trans. Intell. Transp. Syst.*, vol. 23, no. 2, pp. 1009–1018, Feb. 2022.
[27] K. Rusek, J. Suárez-Varela, P. Almasan, P. Barlet-Ros, and A. Cabellos-Aparicio, "RouteNet: Leveraging graph neural networks for network modeling and optimization in SDN," *IEEE J. Sel. Areas Commun.*, vol. 38, no. 10, pp. 2260–2270, Oct. 2020.
[28] T. Li, S. Leng, Z. Wang, K. Zhang, and L. Zhou, "Intelligent resource allocation schemes for UAV-swarm-based cooperative sensing," *IEEE Internet Things J.*, vol. 9, no. 21, pp. 21570–21582, Nov. 2022.
[29] S. Scardapane, I. Spinelli, and P. D. Lorenzo, "Distributed training of graph convolutional networks," *IEEE Trans. Signal Inf. Process. Netw.*, vol. 7, pp. 87–100, 2021.
[30] Z. Qin, H. Yao, and T. Mai, "Traffic optimization in satellites communications: A multi-agent reinforcement learning approach," in *Proc. Int. Wireless Commun. Mobile Comput. (IWCMC)*, Jun. 2020, pp. 269–273.
[31] J. Filar and K. Vrieze, *Competitive Markov Decision Processes*. New York, NY, USA: Springer, 2012.
[32] E. V. Denardo, "Contraction mappings in the theory underlying dynamic programming," *SIAM Rev.*, vol. 9, no. 2, pp. 165–177, Apr. 1967.
[33] D. Blakely, J. Lanchantin, and Y. Qi, "Time and space complexity of graph convolutional networks," GitHub, San Francisco, CA, USA. Accessed: Dec. 31, 2021.
[34] X. Hui, J. Bian, Y. Yu, X. Zhao, and M. Tan, "A novel autonomous navigation approach for UAV power line inspection," in *Proc. IEEE ROBIO*, Dec. 2017, pp. 634–639.
[35] M. Ravanelli, T. Parcollet, and Y. Bengio, "The PyTorch-Kaldi speech recognition toolkit," in *Proc. ICASSP*, May 2019, pp. 6465–6469.
[36] H. Qinghua, P. Minghai, Z. Wucai, and L. Zhiheng, "Time resource management of OAR based on fuzzy logic priority for multiple target tracking," *J. Syst. Eng. Electron.*, vol. 29, no. 4, pp. 742–755, Aug. 2018.
[37] W. Chen et al., "MADDPG algorithm for coordinated welding of multiple robots," in *Proc. 6th Int. CACRE*, Jul. 2021, pp. 1–5.
[38] Y. Yu et al., "Distributed multi-agent target tracking: A Nash-combined adaptive differential evolution method for UAV systems," *IEEE Trans. Veh. Technol.*, vol. 70, no. 8, pp. 8122–8133, Aug. 2021.
[39] Z. Xia et al., "Multi-agent reinforcement learning aided intelligent UAV swarm for target tracking," *IEEE Trans. Veh. Technol.*, vol. 71, no. 1, pp. 931–945, Jan. 2022.
[40] X. Zhu, S. Lyu, X. Wang, and Q. Zhao, "TPH-YOLOv5: Improved YOLOv5 based on transformer prediction head for object detection on drone-captured scenarios," in *Proc. IEEE/CVF Int. Conf. Comput. Vis. Workshops (ICCVW)*, Oct. 2021, pp. 2778–2788.
[41] B. B. Bhagat and A. B. Raj, "Detection of human presence using UWB radar," in *Proc. ICSCAN*, Jul. 2021, pp. 1–6.

Longyu Zhou (Student Member, IEEE) is currently pursuing the Ph.D. degree with the School of Information and Communication Engineering, University of Electronic Science and Technology of China (UESTC).

He is a Visiting Student with the Embedded and Networking System (ENS) Group, Delft University of Technology, The Netherlands. His research interests include the Internet of Things, edge intelligence, resource scheduling, and wireless sensor networks. He also serves/has served as a TPC Member for the IEEE International Conference on Communications (ICC) and IEEE ICCC Workshop. He was a recipient of the Best Paper Award from the 20th IEEE International Conference on Communications and Technology. He also serves/has served as a reviewer for the IEEE INTERNET OF THINGS JOURNAL, the IEEE TRANSACTIONS ON VEHICULAR TECHNOLOGY, and the IEEE Global Communications Conference (GLOBECOM).

Supeng Leng (Member, IEEE) received the Ph.D. degree from Nanyang Technological University (NTU), Singapore. He has been a Research Fellow with the Network Technology Research Center, NTU. He is currently a Full Professor with the School of Information and Communication Engineering, University of Electronic Science and Technology of China (UESTC). He is also the Leader of the Research Group, Ubiquitous Wireless Networks. He has published over 150 research articles in recent years. His research interests include spectrum, energy, routing and networking in the Internet of Things, vehicular networks, broadband wireless access networks, smart grids, and next-generation mobile networks. He serves as an organizing committee chair and a TPC member for many international conferences. He serves as a reviewer for over ten international research journal articles.

Qing Wang (Senior Member, IEEE) received the Ph.D. degree from UC3M and the IMDEA Networks Institute, Spain, in 2016. He is currently an Assistant Professor with the Embedded and Networked Systems Group, Delft University of Technology, The Netherlands. He is also the Co-Founder of OpenVLC, an open-source and low-cost platform for VLC research. His research outcomes on active/passive visible light communication and sensing systems have been published in IEEE/ACM conference papers and journal articles, such as ACM MobiCom, CoNEXT, SenSys, IEEE INFOCOM, IEEE/ACM TRANSACTIONS ON NETWORKING, and IEEE JOURNAL ON SELECTED AREAS IN COMMUNICATIONS. His research interests include visible light communication and sensing systems, and the Internet of Things. He has received several awards, including the MobiCom Honourable Mention Award in 2020, the COMSNETS Best Paper Award in 2019, the Accenture Innovation Award in 2017, and the Best Paper Runner-Up at CoNEXT in 2016.

Yujun Ming received the dual B.S. degrees in communication engineering from the University of Glasgow, Glasgow, U.K., and the University of Electronic Science and Technology of China (UESTC), Chengdu, China, in 2021. She is currently pursuing the M.S. degree with the School of Information and Communication Engineering, UESTC. Her research interests include vehicular networks, multi-agent systems, and the Internet of Things.

Qiang Liu (Member, IEEE) received the B.S., M.S., and Ph.D. degrees from the University of Electronic Science and Technology of China (UESTC), China, in 1996, 2000, and 2012, respectively. After graduating from the M.S. study in 2000, he was with the School of Communication and Information Engineering, UESTC, where he is currently a Full Professor. He was with the University of Essex, U.K., from December 2012 to December 2013, and the University of California at Davis, Davis, CA, USA, from August 2017 to August 2018, as a Visitor Scholar. His research interests include wireless sensor networks, the Internet of Things, broadband wireless networks, and molecular communication. He is a member of IEEE ComSoc. He is a reviewer of IEEE TRANSACTIONS ON NANOBIOSCIENCE and *International Journal of Communication Systems* (IJCS).